



Cu-Mn Bimetallic Complex Immobilized on Magnetic NPs as an Efficient Catalyst for Domino One-Pot Preparation of Benzimidazole and Biginelli Reactions from Alcohols

Mohammad Ali Nasseri¹ · Zinat Rezazadeh¹ · Milad Kazemnejadi¹ · Ali Allahresani¹

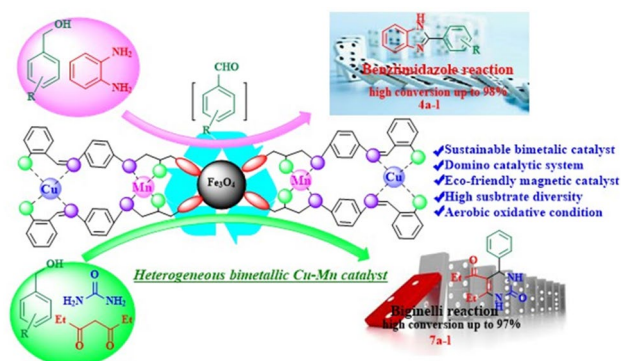
Received: 19 May 2020 / Accepted: 28 August 2020
© Springer Science+Business Media, LLC, part of Springer Nature 2020

Abstract

An efficient magnetically recyclable bimetallic catalyst by anchoring copper and manganese complexes on the Fe_3O_4 NPs was prepared and named as $\text{Fe}_3\text{O}_4@\text{Cu-Mn}$. It was found as a powerful catalyst for the domino one-pot oxidative benzimidazole and Biginelli reactions from benzyl alcohols as a green protocol in the presence of air, under solvent-free and mild conditions. $\text{Fe}_3\text{O}_4@\text{Cu-Mn}$ NPs were well characterized by FT-IR, XRD, FE-SEM, TEM, VSM, TGA, EDX, DLS, and ICP analyses. The optimum range of parameters such as time, temperature, amount of catalyst, and solvent were investigated for the domino one-pot benzimidazole and Biginelli reactions to find the optimum reaction conditions. The catalyst was compatible with a variety of benzyl alcohols, which provides favorable products with good to high yields for all of derivatives. Hot filtration and Hg poisoning tests from the nanocatalyst revealed the stability, low metal leaching and heterogeneous nature of the catalyst. To prove the synergistic and cooperative effect of the catalytic system, the various homologues of the catalyst were prepared and then applied to a model reaction separately. Finally, the catalyst could be filtered from the reaction mixture simply, and reused for five consecutive cycles with a minimum loss in catalytic activity and performance.

Graphic Abstract

A new magnetically recyclable Cu/Mn bimetallic catalyst has been developed for domino one-pot oxidation-condensation of benzimidazole and Biginelli reactions from alcohols.



Keywords Bimetallic catalyst · $\text{Fe}_3\text{O}_4@\text{Cu-Mn}$ · One-pot multicomponent reactions · Benzyl alcohols

Electronic supplementary material The online version of this article (<https://doi.org/10.1007/s10562-020-03371-0>) contains supplementary material, which is available to authorized users.

✉ Mohammad Ali Nasseri
manaseri@birjand.ac.ir

Extended author information available on the last page of the article

1 Introduction

Most sustainable intermediates have resulted from multicomponent reactions as a key synthetic method due to obvious advantages including synthetic efficiency and

molecular diversity. Among all these type of reactions, Biginelli and benzimidazole reactions were highly regarded due to the most robust biological and therapeutic activities [1, 2]. Dihydropyrimidinones (DHPMs) and their derivatives have been found to revolutionize situation in synthetic methodologies that so-called Biginelli reaction. Biginelli is a cyclo-condensation reaction which synthesized carbonyl components in the strong acidic medium [3–7]. On the other hand, benzimidazoles are heterocyclic aromatic compounds containing fused benzene and imidazole rings. Benzimidazoles are effective bicyclic compounds for pharmaceutical purposes such as anticancer, antifungal, and anti-virus activities [7–12], that prepared from aldehydes and *o*-phenylenediamines under vigorous conditions. These are valuable techniques for the synthesis of simple to complicate bicyclic compounds which have been found various potential applications such as biological activity, optical properties, thermos-stability, asymmetric synthesis, and combinatorial chemistry [13–15]. Hence, the preparation of dihydropyrimidinones and benzimidazoles are highlighted in the reports. On the other hand, carbonyl scaffolds play vital role because of distinct features in different science aspects including pharmacy, vitamin syntheses, perfuming industry, organic synthesis, and tandem reactions. After polymerization reactions, oxidations have been found the second circumstances in the chemical industries [16]. Selective oxidation of alcohols to carbonyl are a category of chemical transformation under aerobic conditions as a non-toxic, cheap, and safe oxidant. From the environmentally and atom economy viewpoint, alcohols as the versatile, renewable, sustainable, affordable, diverse, and abundant resources have received great attention from engineers and scientists [16–20].

In spite of carbonyl compounds validity, considerable reactions including Strecker, Hantzsch, Biginelli, Mannich, Passerini, Ugi, *N*-heteroatom bicyclic, and etc. were handled with these intermediates. Classical methods are based on substrate interactions from elaboration carbonyl compounds as more volatile, toxic, unstable, and more expensive. To address this impediment, using alcohol derivatives is a benign strategy in cascade reactions. Domino reactions are facile, economic, and ecological rather than stepwise models. In this way, multicomponent reactions have been considered by the domino catalytic systems such as Biginelli, Knoevenagel, benzimidazole, and pyridine rings synthesis [21–25]. Thus, the replacement of the direct synthesis by multi-step one, are manifold advantages for environmental and industrial goals such as renewable materials, high atom economy, and eco-friendly nature.

Metal-based catalysts rather than traditional oxidants founded special places in aerobic alcohol oxidations [26, 27]. Pivotal roles of metal-based catalysts in this field are removal of toxic Cr(VI) and Mn(VII), decreasing by-product, high E-factor (mass of waste/mass of product), immense

scale-up, and increasing chemoselectivity in aerobic conditions. To overcome these problems, catalytic systems based Cu, Rh, Pd, Fe, Au, Vo, Ir, and Mn introduced as an emerging alternative method. Industrial point of view, high selectivity, high efficiency, mild conditions, affordable, and energy saving were important goals to achieve with the metal based catalytic systems in aerobic conditions [26–31].

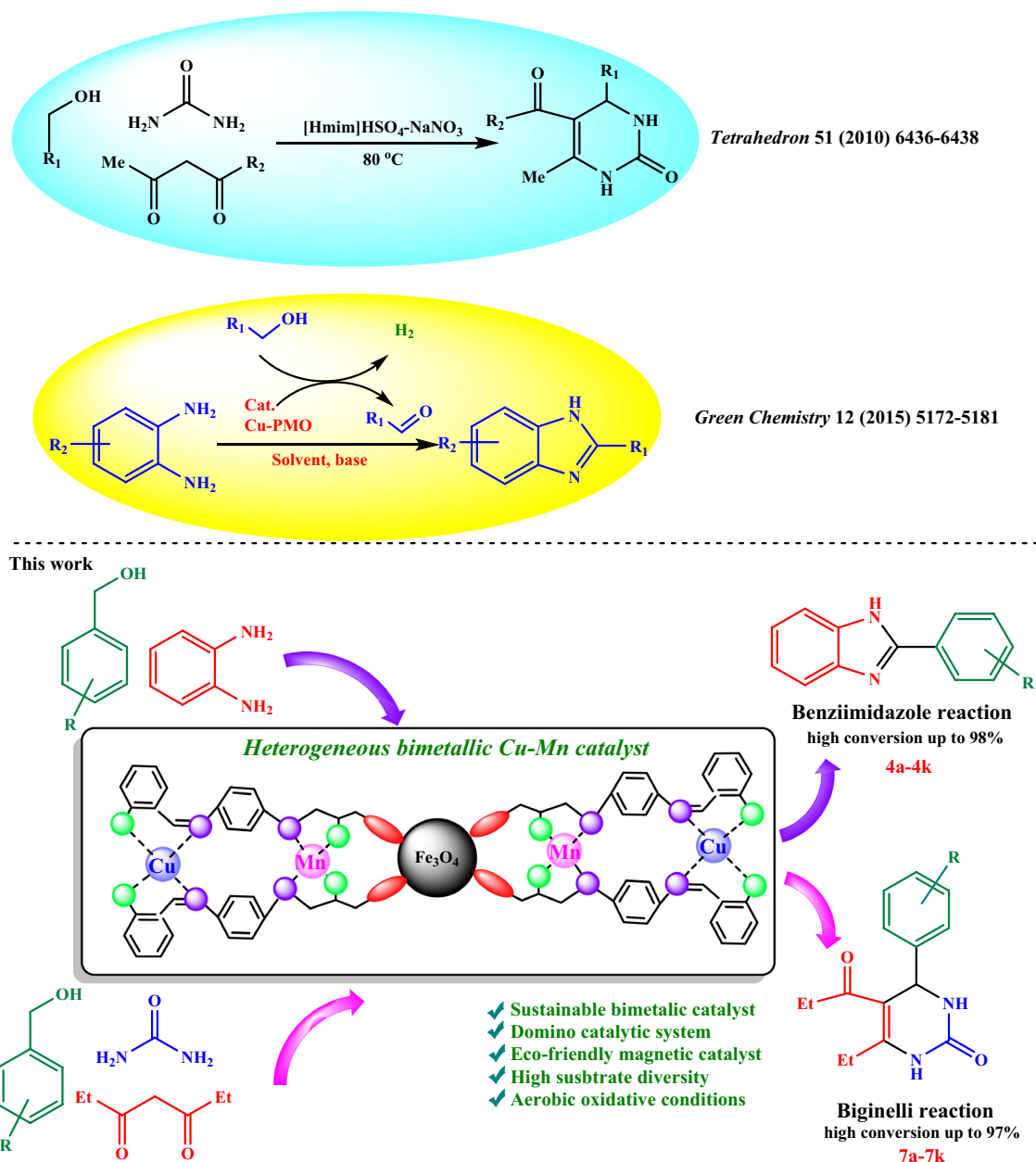
Moreover, the design of bimetallic catalysts for aza-heterocycle synthesis is clever mindful due to the specific properties such as cooperativity effect, chemoselectivity, high reaction rate, cost-effective, and two available active sites. So pioneering bimetallic catalysts could be handle one-pot reactions to obtain a target product with high yield, high selectivity, low reaction time, and removal of purification/separation step for the intermediates. Thus, energy saving and the ultimate cost reduction of the product are advantages of these catalysts in the cascade reactions, definitely [32–34]. In this regard, various bimetallic systems reported for a variety of organic reactions such as multi component, cross coupling, and domino one-pot reactions [35–39]. Wang et al. introduced a catalytic performance system as name as Pd_xNi_y@ZIF-8 for Sonogashira cross-coupling, which synergistic effect studied between Pd and Ni in the efficiency and catalyst activity [40]. A novel Al-Ti bimetal incorporated 3D mesoporous TUD-1 reported by Pasupathi et al. for Biginelli reaction under mild reactions. The researchers suggested a plausible mechanism based on Al³⁺ and Ti⁴⁺ ions for the preparation of the 3,4-dihydropyrimidinones [41]. Kamjijo et al. illustrated the synthesis of various triazoles from alkynes using Pd–Cu bimetallic catalyst system [42]. Copper and manganese are two inexpensive and nontoxic noble metals, with high abundance in nature. The well-known Lewis acid activity of Cu and powerful oxidation activity of Mn, make them as suitable metals for the preparation of a bimetallic catalytic system for domino oxidation-condensation reactions.

In this study, we synthesized a magnetically recyclable Copper/Manganese bimetallic nanocatalyst (Fe₃O₄@Cu-Mn) with high performance for domino oxidation-condensation reaction of Biginelli and benzimidazoles from alcohols. Cooperatively and synergetic effects in Fe₃O₄@Cu-Mn were investigated with various control experiments (Scheme 1).

2 Experimental

2.1 Material and Instruments

All materials were purchased from Sigma and Fluka suppliers and used without further treatment. The distilled and dried solvents were used for all reactions. The analytical grade was selected for all other reagents. Thin layer



Scheme 1. The Chemical structure of Fe_3O_4 @Cu-Mn bimetallic catalytic system for green one-pot Biginelli and benzimidazole reactions from benzyl alcohols

chromatography (TLC) was performed for monitoring reaction progress. FTIR spectra were obtained using a JASCO FT/IR 4600 spectrophotometer using KBr pellet. The ^1H NMR (250 MHz) and ^{13}C NMR (62.9 MHz) spectra were recorded on a Bruker Avance DPX-250 spectrometer in the deuterated solvents (CDCl_3 and $\text{DMSO}-d_6$) and TMS as an internal standard. Field emission scanning electron microscopy (FE-SEM) images were achieved on a SEM FEI Quanta 200. Gas chromatography (GC) analyses were performed using a Shimadzu-14B gas chromatograph equipped with an HP-1 capillary column and N_2 as a carrier

gas. Anisole was used as the internal standard. EDX analyses were performed using a FESEM, JEOL 7600F apparatus equipped with a spectrometer of energy dispersion of X-Ray from Oxford instruments. TEM microscopic images were performed on a Philips EM208S microscope operated at 100 kV. TGA analyses of the samples were performed on a Q600 model from TA company made in U.S.A under nitrogen atmosphere with a heating rate of $10\text{ }^\circ\text{C}/\text{min}$, and in the temperature range of $25\text{--}1000\text{ }^\circ\text{C}$. VSM curve of the samples was analyzed on a Lake Shore Cryotronics 7407 at room temperature. ICP experiments were conducted using a

VARIAN VISTA-PRO CCD simultaneous ICP-OES instrument. XRD patterns were obtained on a Rigaku SmartLab instrument. The size distribution of the nanoparticles was measured using the dynamic light scattering (DLS) method using a HORIBA-LB550 instrument.

2.2 Preparation of Fe₃O₄@Epoxide (i)

The Fe₃O₄ magnetic nanoparticles were synthesized according to a previously reported procedure [43]. After dispersion of Fe₃O₄ NPs (0.5 g) in 10 ml DMSO, 5.0 mmol trimethylamine (Et₃N) was added dropwise to the dispersed solution, then epichlorohydrin (5.0 mmol) was added to the mixture at 90 °C in an oil bath. The mixture was stirred for 48 h under N₂ atmosphere. The Fe₃O₄@Epoxide product was separated by a permanent magnetic field and washed three times with absolute ethanol. The resulted nanoparticles were dried overnight, then characterized by FT-IR, and EDX analyses (Table 1).

2.3 Preparation of Fe₃O₄@NH₂ (ii)

In order to functionalize Fe₃O₄@Epoxide with NH₂ groups, a mixture of Fe₃O₄@Epoxide (0.5 g) and 5.0 mmol *p*-phenylenediamine were stirred in 10 ml DMSO extremely in the presence of Et₃N (5.0 mmol) at 60 °C for 24 h. The desired product **ii** (Scheme 2) was separated by an external magnet, repeatedly washed with ethanol to remove unreacted materials, then dried overnight. The product was characterized by FT-IR and EDX analyses (Table 1).

The coordination of Mn ions to the magnetic NPs (**ii**) was performed via the mixing of Fe₃O₄@NH₂ (0.5 g) with 1.0 mmol manganese(II) acetate in ethanol at 60 °C for 4 h. Then, Fe₃O₄@epoxide-Mn complex was magnetically separated, washed with deionized water and ethanol (3 × 12 mL),

and dried in a vacuum oven. Fe₃O₄@Mn-NH₂ (compound **iii**, Scheme 2) was characterized by FT-IR and EDX analyses (Table 1).

To prepare the Cu–Mn bimetallic catalyst, a Schiff base moiety as a secondary ligand was designed in compound (**iii**) structure through the mixing compound **iii** (0.5 g) and 5.0 mmol salicylaldehyde in ethanol at room temperature for 4 h. The obtained solid was separated and washed repeatedly (**iv**, Scheme 2). The Fe₃O₄@NH₂-Mn-SB (compound **iv**) was characterized by FT-IR and EDX analyses (Table 1).

2.4 Preparation Route of Fe₃O₄@Cu-Mn Catalyst (v)

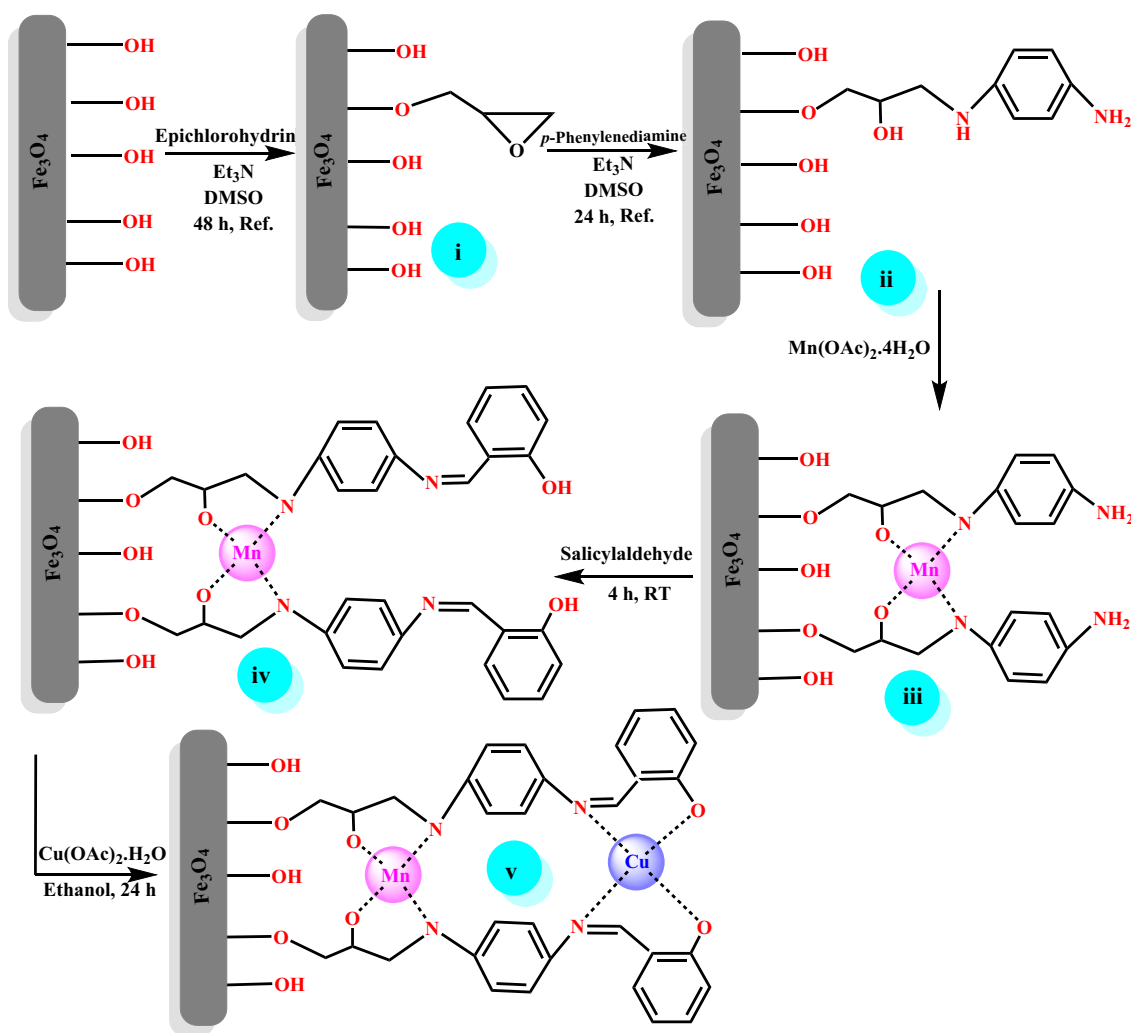
Compound **iv** (0.5 g) and 0.1 g Cu(OAc)₂·H₂O was suspended in 20 ml absolute ethanol then sonicated until it became completely dispersed. Subsequently, the mixture was stirred for 24 h at 60 °C under air atmosphere. The resulting solid product (**v**) was separated and washed. The product was characterized by FT-IR, and EDX analyses (Table 1). Scheme 2 shows the general synthetic approach for the preparation of **i**, **ii**, **iii**, **iv**, and **v**.

2.5 General Procedure for Domino One-Pot Preparation of Benzimidazole and Biginelli Derivatives Catalyzed by Fe₃O₄@Cu-Mn

The one-pot synthesis of benzimidazole carried out in a round-bottom flask with benzyl alcohol (1.2 mmol) and *ortho* phenylenediamine (1.0 mmol) using Fe₃O₄@Cu-Mn catalyst (0.008 g, 0.280 mol% **Cu**, 0.078 mol% **Mn**), under solvent-free and aerobic conditions at 70 °C. The reaction mixture was monitored with TLC. Upon reaction completion, the catalyst was magnetically separated, then the product was extracted to dichloromethane (3 × 5 mL). The organic layers were combined, dried over Na₂SO₄ and

Table 1 Representative data of the synthesized compounds

Compound	FT-IR & EDX data
i	IR (KBr): ν (cm ⁻¹) = 502 (Fe–O–Fe stretching), 635, 733, 1102 (asymmetric and symmetric stretching of epoxide ring), 3249 (OH band). EDX analysis: Fe = 40.32%wt, O = 36.19%wt, C = 23.48%wt (†ESI, Figure S1, S2)
ii	IR (KBr): ν (cm ⁻¹) = 518 (Fe–O–Fe stretching), 1043 (C–O stretching), 1480 (Ph), 1596 (Ph), 2920 (CH- <i>sp</i> ₃), 2960 (CH- <i>sp</i> ₂), 3251, 3303 (NH ₂ stretching), 3372 (OH band). EDX analysis: Fe = 37.31%wt, O = 34.40%wt, N = 5.08%wt, C = 23.21%wt (†ESI, Figure S1, S3)
iii	IR (KBr): ν (cm ⁻¹) = 481 (Fe–O–Fe stretching), 635 (Mn–O stretching), 698 (Mn–N stretching), 1019 (C–O stretching), 1339 (Ph), 1590 (Ph), 2926 (CH- <i>sp</i> ₃), 2980 (CH- <i>sp</i> ₂), 3367 (OH band). EDX analysis: Fe = 18.53%wt, O = 50.26%wt, N = 3.71%wt, C = 16.08%wt, Mn = 11.42%wt (†ESI, Figure S1, S4)
iv	IR (KBr): ν (cm ⁻¹) = 505 (Fe–O–Fe stretching), 620 (Mn–O stretching), 631 (Mn–N stretching), 1016 (C–O stretching), 1150 (C–N stretching), 1370 (Ph), 1585 (Ph), 1650 (C=N stretching), 2852 (CH- <i>sp</i> ₃), 2922 (CH- <i>sp</i> ₂), 3370 (OH band). EDX analysis: Fe = 24.17%wt, O = 41.17%wt, N = 3.65%wt, C = 23.71%wt, Mn = 7.30%wt (†ESI, Figure S1, S5)
v	IR (KBr): ν (cm ⁻¹) = 484 (Fe–O–Fe stretching), 560 (Cu–O stretching), 633 (Mn–O and Cu–N stretching), 676 (Mn–N stretching), 1032 (C–O stretching), 1132 (C–N stretching), 1339 (Ph), 1530 (Ph), 1620 (C=N stretching), 2928 (CH- <i>sp</i> ₃), 2980 (CH- <i>sp</i> ₂), 3367 (OH band). EDX analysis: Fe = 24.58%wt, O = 41.28%wt, N = 10.10%wt, C = 21.28%wt, Mn = 0.54%wt, Cu = 2.23%wt (†ESI, Figure S1)



Scheme 2 The general synthetic approach for preparation of the $\text{Fe}_3\text{O}_4@Cu-Mn$

purified by silica-gel column chromatography (*n*-hexane: EtOAc = 10: 5).

For the Biginelli reaction, benzyl alcohol (1.2 mmol), ethyl acetoacetate (1.2 mmol), and urea (1.0 mmol) were reacted in the presence of $\text{Fe}_3\text{O}_4@Cu-Mn$ catalyst (0.008 g, 0.280 mol% Cu, 0.078 mol% Mn) under solvent-free and aerobic conditions at 70 °C. Repeatedly, the reaction performance and product purification was as same as the benzimidazole reaction. After the reaction completion, the magnetic catalyst was separated easily by an external magnet and the product was extracted to dichloromethane (3 × 5 mL). The organic layers were combined, dried over Na_2SO_4 and purified by silica-gel column chromatography (*n*-hexane: EtOAc = 12: 3). The products were characterized and identified by comparing their melting point and NMR analyses with those authentic samples.

3 Result and Discussion

The catalyst, $\text{Fe}_3\text{O}_4@Cu-Mn$, was characterized step by step by FT-IR analysis to investigate its structure and formation of the desired bands. The FT-IR spectra of the compounds **i**, **ii**, **iii**, **iv**, and $\text{Fe}_3\text{O}_4@Cu-Mn$ (**v**) was shown in Fig. 1. As shown in Fig. 1, the characteristic peaks at 502 cm^{-1} , 635 cm^{-1} , 733 cm^{-1} , 1102 cm^{-1} , and 3249 cm^{-1} represent the absorptions correspond to Fe–O–Fe (Stretching vibration), C–O–C asymmetric and symmetric stretching of epoxide ring, and the broad O–H band (stretching vibration) respectively, which confirms the structure of compound **i** (Fig. 1) [44]. FT-IR spectrum of **ii** exhibited the absorption bands at 518 cm^{-1} (Fe–O–Fe stretching), 1043 cm^{-1} (C–O stretching), 1480 cm^{-1} (Ph), 1596 cm^{-1} (Ph), 2920 cm^{-1} ($\text{CH-}sp^3$), 2960 cm^{-1} ($\text{CH-}sp^2$), 3251 , 3303 cm^{-1} (NH_2 stretching), and 3372 cm^{-1} (OH band). These absorption bands confirmed the successful preparation of **ii** with the

amine groups. The presence of the bands at 635 cm^{-1} (Mn–O stretching), 698 cm^{-1} (Mn–N stretching) in the FT-IR spectrum of **iii**, clearly represents the formation of the manganese complex [45, 46]. Figure 1 shows the FTIR spectrum **iv** with three characteristic peaks at 620, 631, and 1650 cm^{-1} related to Mn–O, Mn–N and C=N stretching bands respectively, that approves the formation of $\text{Fe}_3\text{O}_4@ \text{NH}_2\text{-Mn-SB}$ nanoparticles [47]. The imine band absorption (1650 cm^{-1}) shifted to higher wavenumbers (1620 cm^{-1}) in the Cu–Mn bimetallic catalyst spectrum (compound **v**). Also, three absorption bands at 560, 633, and 679 cm^{-1} could be assigned to Cu–O, Cu–N, Mn–O, and Mn–N stretching vibrations respectively [48].

A quite uniform size with a spherical morphology vision was proved by the FE-SEM image of $\text{Fe}_3\text{O}_4@ \text{Cu-Mn}$ nanoparticles (Fig. 2a). As shown in Fig. 2b, the TEM microscopic image verified the spherical morphology and characteristic core–shell for the magnetic bimetallic catalyst with an average size of 24 nm [49]. It is noted that the shape and particle size of the catalyst did not change after functionalization. The size distribution histogram was estimated a mean diameter of 24–26 nm for $\text{Fe}_3\text{O}_4@ \text{Cu-Mn}$ nanoparticles, which presented relatively narrow size distribution (Fig. 2c).

The catalyst was characterized step by step by EDX analysis to investigate the structure and the presence of the expected elements (Fig. 3 and †ESI, Fig. S1–S4). To obtain more precise data about the amount of elements, the EDX analyses were taken from the compound **i**, **ii**, **iii**, **iv**, and **v**. EDX analysis was proved the removal of chloride for $\text{Fe}_3\text{O}_4@ \text{Epoxide}$ (compound **i**) structure. The elements including carbon, nitrogen, oxygen, iron, and manganese confirmed the expected structures for compounds **ii**, **iii**, as the manganese complexes, and also Schiff base complex (compound **iv**). The results confirmed all the expected elements including Fe, O, C, Cu, Mn, and N with 24.58, 41.28, 21.28, 2.23, 0.54, 10.10 wt% values, respectively. The expected elements such as copper and manganese with specified percentages confirmed the preparation of the bimetallic Cu–Mn system.

Figure 4a shows the thermal behavior of the Fe_3O_4 and $\text{Fe}_3\text{O}_4@ \text{Cu-Mn}$ NPs by TGA analysis. The Fe_3O_4 nanoparticles showed only 4.89% weight loss which can be directly related to the trapped water in the nanoparticles crystal structure ($25\text{ }^\circ\text{C}$ – $1000\text{ }^\circ\text{C}$). The TGA curve of $\text{Fe}_3\text{O}_4@ \text{Cu-Mn}$ NPs illustrated about 40% weight loss between $25\text{ }^\circ\text{C}$ and $1000\text{ }^\circ\text{C}$. In addition, removal of the adsorbed water on the surface of the catalyst and trapped water in the crystal structure occur at below $200\text{ }^\circ\text{C}$ and $350\text{ }^\circ\text{C}$, respectively. Another two weight losses revealed the removal of Schiff base ligands and different organic groups immobilized on NPs, which proved the successful grafting of the bimetallic complex onto the magnetite surface. The TGA curve of the bimetallic $\text{Fe}_3\text{O}_4@ \text{Cu-Mn}$ nanoparticles shows

a continuous weight loss with a mild slope up to $\sim 450\text{ }^\circ\text{C}$ (~ 6.49 weight loss), indicating the decomposition of Schiff base ligands [50]. Significant weight loss occurs at $\sim 708\text{ }^\circ\text{C}$ with a $\sim 16.43\%$ weight loss (sharp slope), which is related to the decomposition of different organic fragments on the nanoparticles surface.

VSM analyses revealed the magnetic behavior of Fe_3O_4 and $\text{Fe}_3\text{O}_4@ \text{Cu-Mn}$ NPs (Fig. 4b). The saturation magnetization for Fe_3O_4 and $\text{Fe}_3\text{O}_4@ \text{Cu-Mn}$ catalysts were determined as 74.28 and 56.80 emu/g respectively. Zero coercivity for the nanoparticles with no hysteresis loop indicates the superparamagnetic properties of the NPs. The magnetization decrease of 17.48 emu/g clearly illustrates the high immobilization of Cu–Mn bimetal section on the Fe_3O_4 NPs without significant change in the magnetic property, although Cu–Mn complex operated as a distorted diamagnetic shell [51]. Despite this reduction, the magnetite bimetallic nanoparticles were well and easily separated from the reaction medium by a simple external magnetic field which could be a prerequisite for magnetic nature of a catalyst.

The six diffraction peaks at $2\theta = 35.18^\circ$, 40.63° , 48.33° , 58.73° , 62.33° , and 67.83° related to respectively (220), (311), (400), (422), (511), and (440) planes, were completely in agreement with the crystal structure of Fe_3O_4 NPs characterized by XRD (JCPDS card no. 19-629) (Fig. 5) [52]. Comparison of XRD patterns of Fe_3O_4 and the catalyst, exhibited that the crystalline phase and peak location related to magnetite crystal structure remained intact during organic loading (functionalization), which confirmed the chemical stability of the prepared Fe_3O_4 NPs. But, the impressive decrease in peak intensity and peak broadening indicated the loading of the amorphous functionality on the magnetite nanoparticles. This occurrence can also be related to the organic functional loading as an amorphous structure on magnetite NPs, which is also a confirmation for the successful functionalization of the Fe_3O_4 NPs. The crystallinity peak intensity reduction after the functionalization process was perfectly aligned with the VSM and TGA analyses (refer to Fig. 4a, b). In addition, the size of the nanoparticles was also investigated by XRD analysis. The crystallite size was calculated by applying the Scherrer's equation: $D = K\lambda/\beta\cos\theta$, where D is the average diameter, K is Sherrer's constant (0.94 for Cu–K α), λ is ray wavelength, β is the peak width of half-maximum, and θ is the Bragg diffraction angle [47]. According to the results, the size of $\text{Fe}_3\text{O}_4@ \text{Cu-Mn}$ was found to be 42 nm.

3.1 Optimization of Reaction Parameters

To study the multicomponent reactions parameters, time, temperature, and amount of the bimetallic catalyst, as three effective parameters were investigated in various conditions over three model reactions of: (a) aerobic oxidation

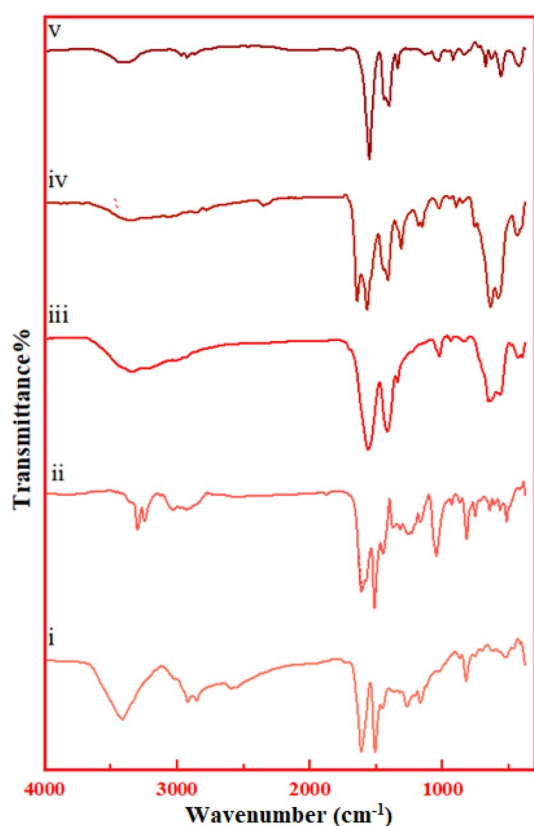


Fig. 1 FT-IR spectra, (i) Fe_3O_4 @Epoxy, (ii) Fe_3O_4 @ NH_2 , (iii) Fe_3O_4 @Epi- Mn- NH_2 , (iv) Fe_3O_4 @Epi- NH_2 -Mn-SB, (v) Fe_3O_4 @Cu-Mn

of benzyl alcohol to aldehyde, (b) benzyl alcohol and *ortho* phenylenediamine (as a benzimidazole reaction model), and (c) benzyl alcohol as well as ethyl acetoacetate with urea as a Biginelli reaction model. The selected premium conditions achieved for the oxidation of benzyl alcohol to benzaldehyde was as, 0.005 g amount of NPs at room temperature for 1.0 h (Table 2, entry 2). Also, the one-pot benzimidazole reaction give high possible efficiency using 0.008 g of NPs, at 70 °C for 2 h (Table 2, entry 13); and the one-pot Biginelli reaction was performed as same as the benzimidazole reaction conditions (Table 2, entry 23). Table 2 shows various conditions tested for the model reactions.

Next, the influence of solvent and oxidant type was evaluated on the model reactions (Fig. 6a and b). The solvent-free conditions had the best effect by providing 93% and 92% efficiency at 70 °C for the one-pot benzimidazole and Biginelli reactions, respectively. The screening results can be justified by the strong interaction of active sites with the reactants in the solvent-free medium (Fig. 6a). Aerobic conditions were provided high yield and then oxidants such as H_2O_2 and O_2 showed moderate to good efficiencies, which is in agreement with the literature for possible electron transfer and contribution between Cu and Mn metals during

oxidative multicomponent processes (Fig. 6b) [38, 53, 54]. Outstandingly, the medium to high efficiencies were established for solvent-free conditions at 70 °C.

In following with the obtained optimum conditions collected in the preceding step, the catalytic activity of Fe_3O_4 @Cu-Mn was investigated in the oxidation of alcohols, one-pot preparation of benzimidazole, and one-pot preparation of Biginelli reactions. Effect of substituted benzylic alcohols for oxidation to aldehydes was investigated by Fe_3O_4 @Cu-Mn (0.178 mol% Cu, 0.049 mol% Mn) at room temperature in ethanol under aerobic conditions (Table 3, 2a–k). Increasing reaction time was observed for benzyl alcohols bearing electron-deficient and more steric hindrance substituent (Table 3, 2b, c and 2j–k). In general, there was no significant difference in the efficiency of alcohols bearing electron-withdrawing and electron donating groups, and good to excellent efficiency was obtained for all derivatives [55].

In following, the catalytic activity of Fe_3O_4 @Cu-Mn was investigated toward benzimidazole reaction (from alcohols) in 80–98% overall yields (Table 4, 4a–4k). Various substituted benzyl alcohols with *ortho* phenylenediamine were condensed in good to excellent yields under solvent-free and aerobic conditions at 70 °C (Table 4). It should be noted that the electron-withdrawing groups on benzyl alcohols (Table 4, entry 4d–4j) reduced the efficiency compared to electron-donating groups (Table 4, 4b and c) [56, 57].

Biginelli reactions were conducted on a variety of benzyl alcohols as well as ethyl acetoacetate with urea by Fe_3O_4 @Cu-Mn (0.280 mol% Cu, 0.078 mol% Mn) at 70 °C under solvent-free conditions in 75–97% overall yields (Table 5, 7a–7k). *Para* substitution benzyl alcohols give satisfactory yields than their corresponding *ortho* substitution, that may be attributed to the steric hindrance effect (Tables 5, 7b, e and c, 1). The electron-donating groups on benzyl alcohols (Table 5, entry 7d–7j) demonstrated more satisfactory yields than the corresponding benzyl alcohol bearing electron-withdrawing groups (Table 5, entry 7b, c) [4, 58].

3.2 Mechanism Study

To elucidate the exact role of the copper and manganese in the catalytic system for domino aerobic oxidative reactions, some control experiments were designed and implemented for the model one-pot Biginelli and benzimidazole reactions under the same reaction conditions (Table 6, entry 1–8). $\text{Cu}(\text{OAc})_2 \cdot \text{H}_2\text{O}$ and $\text{Mn}(\text{OAc})_2 \cdot 4\text{H}_2\text{O}$ didn't give considerable oxidation product (benzaldehyde) under open air conditions, and subsequently a trace amount of benzimidazole and Biginelli was obtained for them (Table 6, entries 1, 2). No catalytic activity was observed for Fe_3O_4 NPs in these conditions (Table 6, entry 3). Among the homologue compounds, efficiency of **iii**, **vi**, and **vii** was worthy and

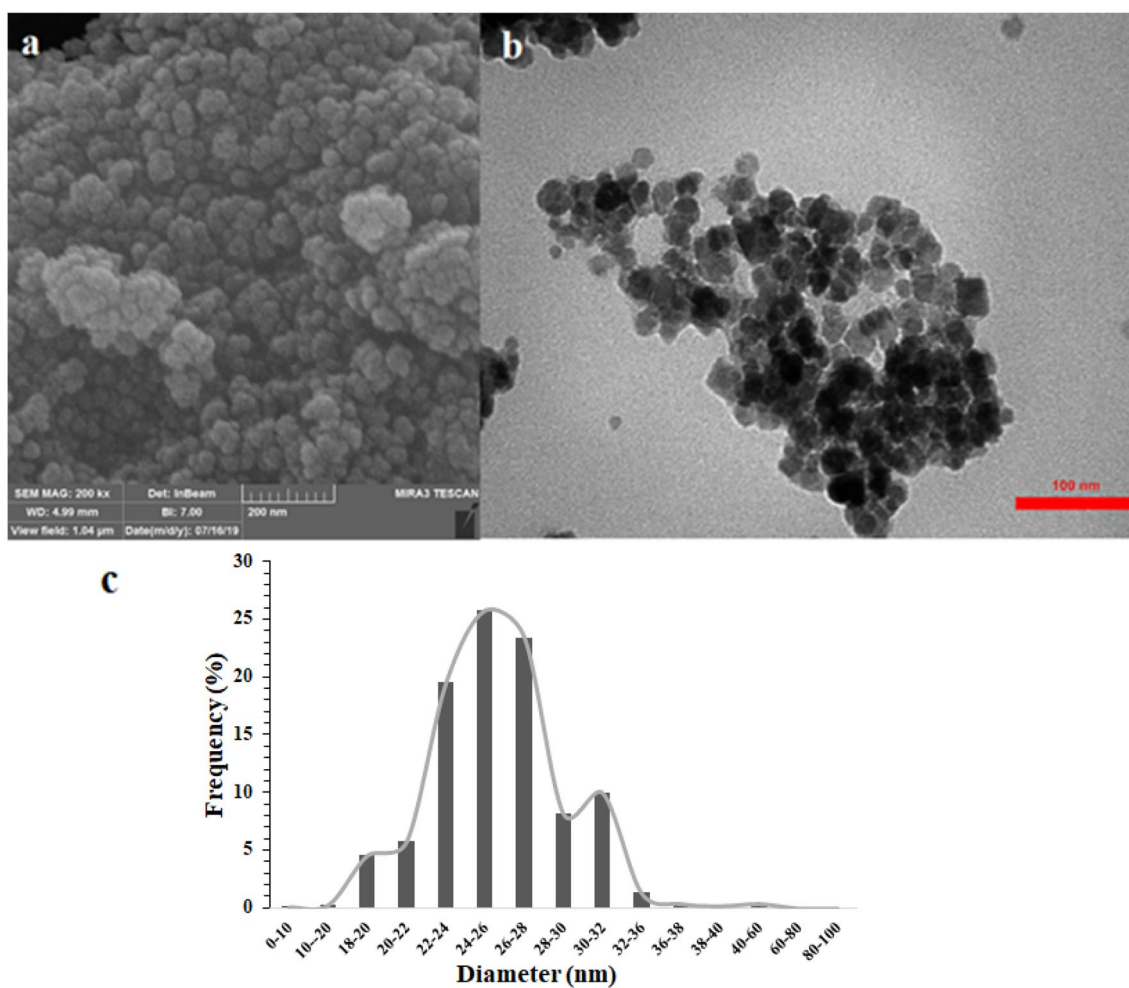


Fig. 2 a FE-SEM, b TEM images, and c size distribution histogram of $\text{Fe}_3\text{O}_4@\text{Cu-Mn}$ NPs

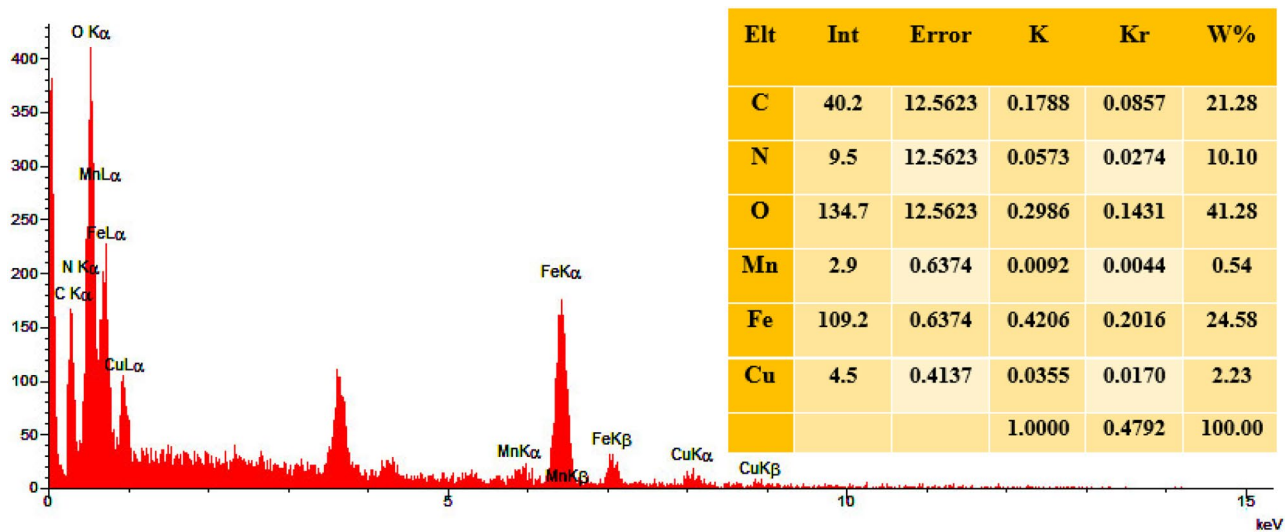


Fig. 3 EDX analysis of $\text{Fe}_3\text{O}_4@\text{Cu-Mn}$

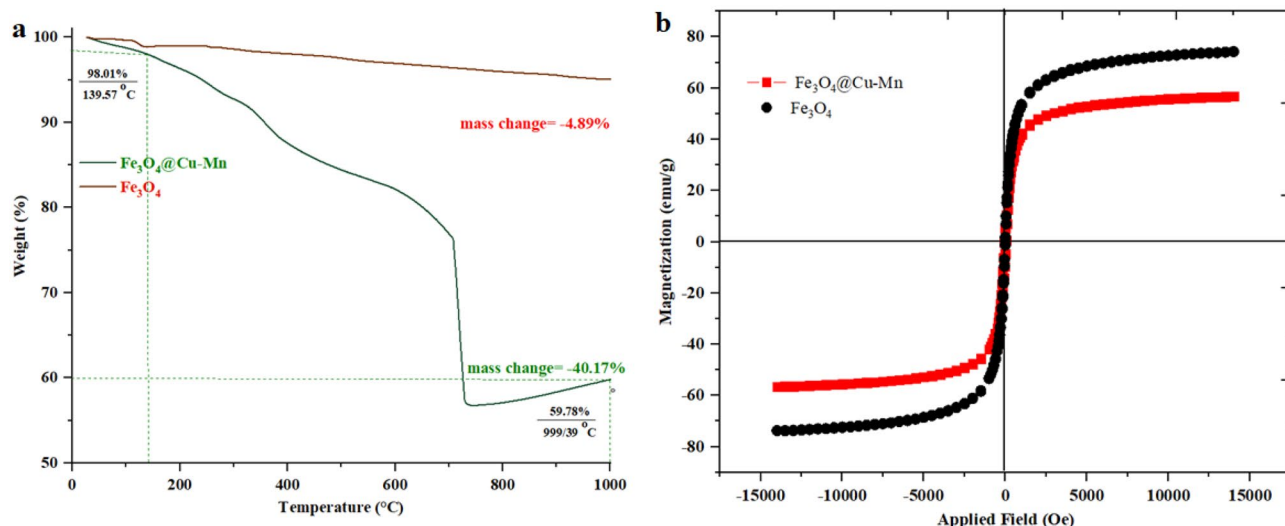


Fig. 4 TGA and VSM curves of Fe_3O_4 @Cu-Mn and Fe_3O_4

impressive (Scheme 3). Oxidation of benzyl alcohol to benzaldehyde by **iii** and **vi** demonstrated a powerful effect of Mn metal (55% yield) compared to Cu metal (35% yield) in the domino oxidative process. As shown in Table 6, manganese majorly performed the oxidation process with higher selectivity (Table 6, entry 4, 5). Moreover, compounds **v** and **vii**, as two bimetallic systems, have shown high selectivity in the oxidation step, which proved the synergistic effect of Cu and Mn centers in the catalyst for the green one-pot reactions of Biginelli and benzimidazole. Finally, compound **v** didn't give any considerable oxidation product (benzaldehyde) under N_2 atmosphere, and a negligible amount of benzimidazole and Biginelli was prepared subsequently (Table 6, entries 8), which demonstrated the cooperative activity of

Cu-Mn bimetallic system for the aerobic (low dependence to molecular oxygen) one-pot process under N_2 atmosphere, and the reaction could be processed somewhat in the absence of any external oxidant. The results clearly manifested the synergistic effect as well as cooperative activity between Mn and Cu for domino oxidation-condensation reaction.

The heterogeneous nature of the catalyst was studied by Hg(0)-poisoning and hot filtration tests over the model one-pot oxidative benzimidazole reaction under optimized conditions. In the filtration test, the catalyst was magnetically recovered after one hour of the reaction. As shown in Fig. 7, after 2 h, the efficiency reached to 60% (GC analysis), indicating the heterogeneous performance of the catalyst in the reaction medium, which no metal leaching occur related to the coordinated Cu or Mn metals in the reaction mixture (Completely consistent with the results of the leaching studies). In addition, in the Hg(0)-poisoning test, mercury(0) was added initially, and in a separate test, it was added after 1 h of reaction time, which 4%, 55% conversion was obtained respectively for the reactions (based on GC analysis). If the catalyst is heterogeneous, the mercury deactivates its activity by poisoning the catalyst (blocks the Cu and Mn active sites) [59] and subsequently the reaction stops. Mercury has no effect on homogeneous catalysts. However, the proposed mechanism is based on previous observations and reports in Table 6 and Fig. 7, wherein the manganese centers were proposed to conduct the reaction via oxidation benzyl alcohols as a Lewis acid and H-bond donor then Copper center developed one-pot Biginelli and benzimidazole directions (Scheme 4) [60–62].

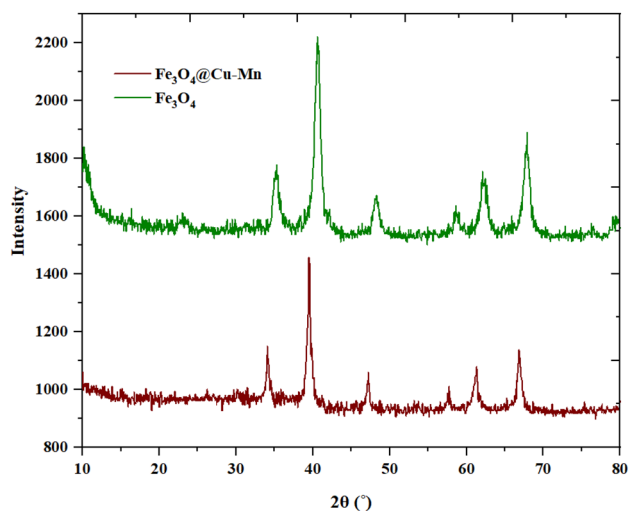


Fig. 5 X-ray diffraction pattern of Fe_3O_4 @Cu-Mn and Fe_3O_4

Table 2 Optimization results for maximum points in the oxidation of alcohols, Biginelli, and benzimidazole one-pot reactions

	Entry	Cu/Mn catalyst (g)	Time (h)	Temperature (°C)	Yield (%)
Oxidation of alcohol to aldehyde ^a	1	0.005	0.5	25	80
	2	0.005	1	25	95
	3	0.005	1.5	25	93
	4	0.005	1	50	92
	5	0.005	1	70	85
	6	0.005	1	90	65
	7	0.006	1	25	91
	8	0.007	1	25	85
	9	0.008	1	25	83
Benzimidazole ^b	10	0.008	0.5	70	40
	11	0.008	1	70	75
	12	0.008	1.5	70	88
	13	0.008	2	70	93
	14	0.008	2.5	70	91
	15	0.008	2	25	65
	16	0.008	2	50	78
	17	0.008	2	90	88
	18	0.009	2	70	91
Biginelli ^c	19	0.01	2	70	89
	20	0.008	0.5	70	52
	21	0.008	1	70	68
	22	0.008	1.5	70	79
	23	0.008	2	70	92
	24	0.008	2.5	70	90
	25	0.008	2	25	56
	26	0.008	2	50	70
	27	0.008	2	90	90
	28	0.009	2	70	89
	29	0.01	2	70	85

^aReaction conditions: Benzyl alcohol (1 mmol), Cat. (0.005 g, 0.175 mol% **Cu**, 0.049 mol% **Mn**), EtOH (2 mL), r.t, open air

^bReaction conditions: Benzyl alcohol (1.2 mmol) and *ortho* phenylenediamine (1 mmol), Cat. (0.008 g, 0.280 mol% **Cu**, 0.078 mol% **Mn**), solvent-free, 70 °C, open air

^cReaction conditions: Benzyl alcohol (1.2 mmol), ethyl acetoacetate (1.2 mmol), and urea (1 mmol), Cat. (0.008 g, 0.280 mol% **Cu**, 0.078 mol% **Mn**), solvent-free, 70 °C, open air

3.3 Proposed Mechanism

According to the proposed mechanism for Lewis acid catalyzed preparation of dihydropyrimidone derivatives, a plausible mechanism was suggested in agreements with the observations and literature for domino one-pot preparation of benzimidazole as well as dihydropyrimidone compounds [63–65]. Given that higher activity of Mn active sites towards alcohol oxidation (Table 6), in first, the alcohol oxidation was carried out with Mn active sites mainly

(Scheme 4). Based on the control experiments, the bimetallic compounds **v**, **vii** provided high selectivity and efficiency than single-metal components under air conditions. The presence of the second metal could be acts as a co-oxidant with a plausible electron exchange [66–68], and subsequently regeneration of the catalyst for the next cycle. In this regard, the Cu and Mn active sites provide a synergistic as well as cooperative performance, which air as a weak oxidant gives a prominent activity. According to the literature, for the preparation of dihydropyrimidone [63], the reaction starts with the coordination of Cu active sites in the catalyst to carbonyl of aldehyde (Intermediate II), then the nucleophilic addition of urea forms intermediate III (Scheme 4). In the next step, the activated β -diketone attacks to the iminium intermediate III and the resulting addition intermediate IV is formed. A cyclization takes place through the nucleophilic addition of amine to carbonyl group, which gives the desired product after removal of a water molecule (Scheme 4). Benzimidazole was also forms via the activation of carbonyl of aldehyde by the catalyst, followed by the nucleophilic addition of *o*-phenylenediamine (Intermediate VI). Finally, a nucleophilic attack of another free amine group causes the formation of benzimidazole ring. It worth noted, that the oxidative activity of the catalyst helps the aromatization of the final intermediate and promotes the efficiency (Table 7).

Finally, the uniqueness of Fe₃O₄@Cu-Mn bimetallic system in the one-pot synthesis of benzimidazole and dihydropyrimidinone derivatives was compared with the recent literatures. The Cu-Mn bimetallic catalyst with the advantages/properties of magnetic, inexpensive, recoverable, and eco-friendly can catalyze the one-pot Biginelli and benzimidazole reactions under open-air and mild conditions with high efficiency.

3.4 Recyclability Studies

In the heterogeneous catalysts field, recovering and recycling of the catalyst are prominent matters for environmental and practical destinations [73]. In this way, the recyclability of the catalyst was studied over the model benzimidazole reaction (between benzyl alcohol and *ortho* phenylenediamine) at 70 °C under open air and solvent-free conditions. As shown in Fig. 8a, the catalyst could be recovered and reused for at least five consecutive times without any notable reduction in catalytic activity. Figure 8a also showed that every recovery yields a very low-efficiency drop, so that after the fifth cycle the efficiency reached to 88%, which is insignificant. In addition, the residual solution after each cycle was studied by ICP analysis to measure metal leaching including Mn and Cu metals. To investigate the stability and structure of the recovered catalyst (after 5th run), it was characterized by FT-IR, FE-SEM, TEM, and TGA analyses (Fig. 8, 9). The FE-SEM and FT-IR analyses of the recovered catalyst also

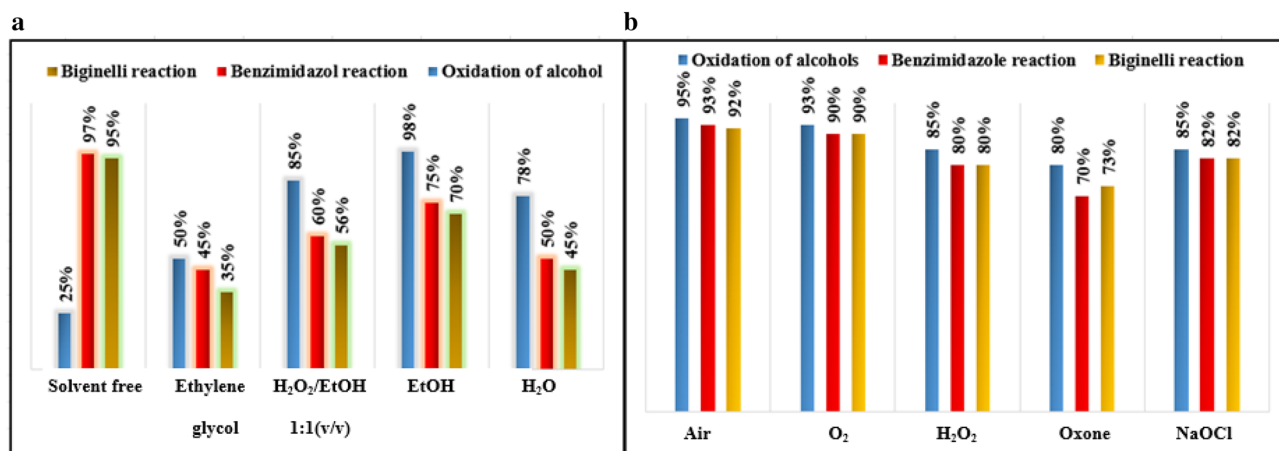


Fig. 6 The screening effect of the **a** solvent, and **b** oxidant on the oxidation of alcohols, benzimidazole, and Biginelli reactions. Reaction conditions: *Biginelli*: Benzyl alcohol (1.2 mmol), ethyl acetate (1.2 mmol), and urea (1 mmol), Cat. (0.008 g, 0.280 mol% **Cu**, 0.078 mol% **Mn**), solvent-free, 70 °C, open air. *Benzimidazole*:

Benzyl alcohol (1.2 mmol), *ortho* phenylenediamine (1 mmol), Cat. (0.008 g, 0.280 mol% **Cu**, 0.078 mol% **Mn**), solvent-free, 70 °C, open air. *Oxidation of alcohols*: Benzyl alcohol (1 mmol), Cat. (0.005 g, 0.175 mol% **Cu**, 0.049 mol% **Mn**), EtOH (2 mL), r.t, open air

Table 3 Oxidation of benzyl alcohols catalyzed by Fe₃O₄@Cu-Mn. Reaction conditions: Benzyl alcohol (1 mmol), Cat. (0.005 g, 0.175 mol% **Cu**, 0.049 mol% **Mn**), EtOH (2 mL), r.t

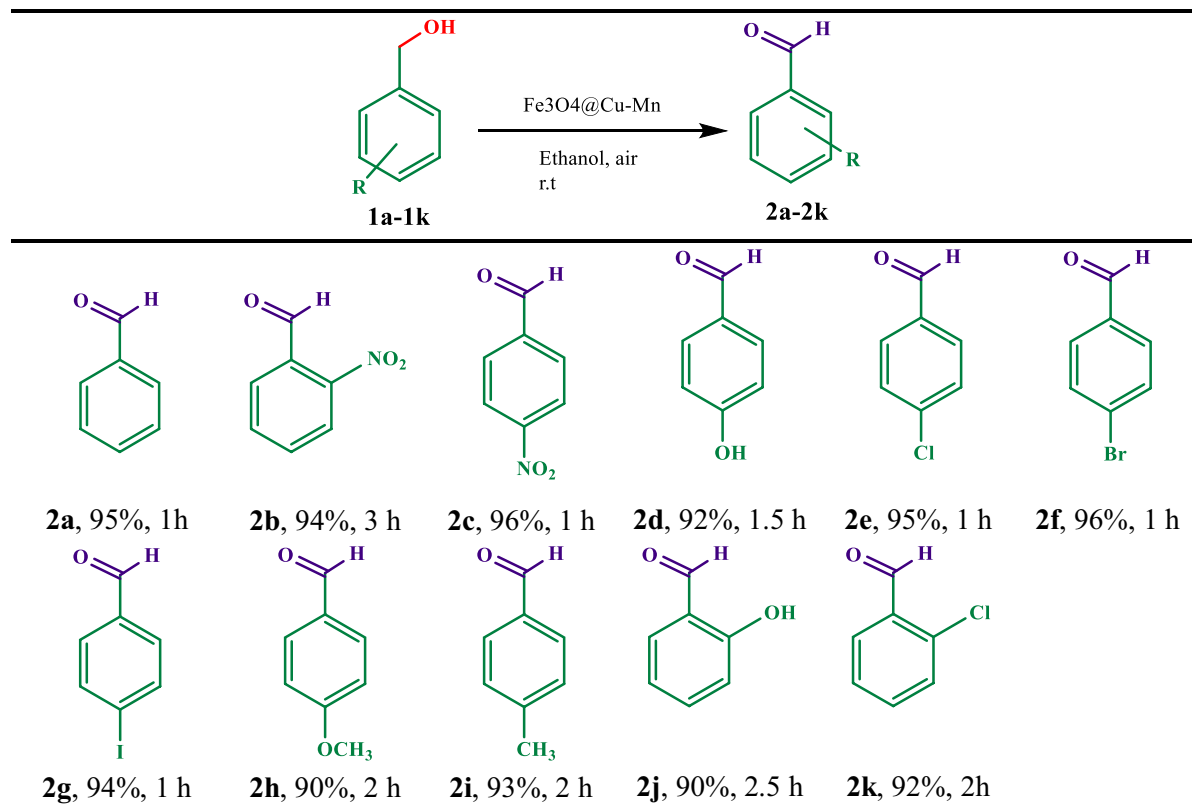
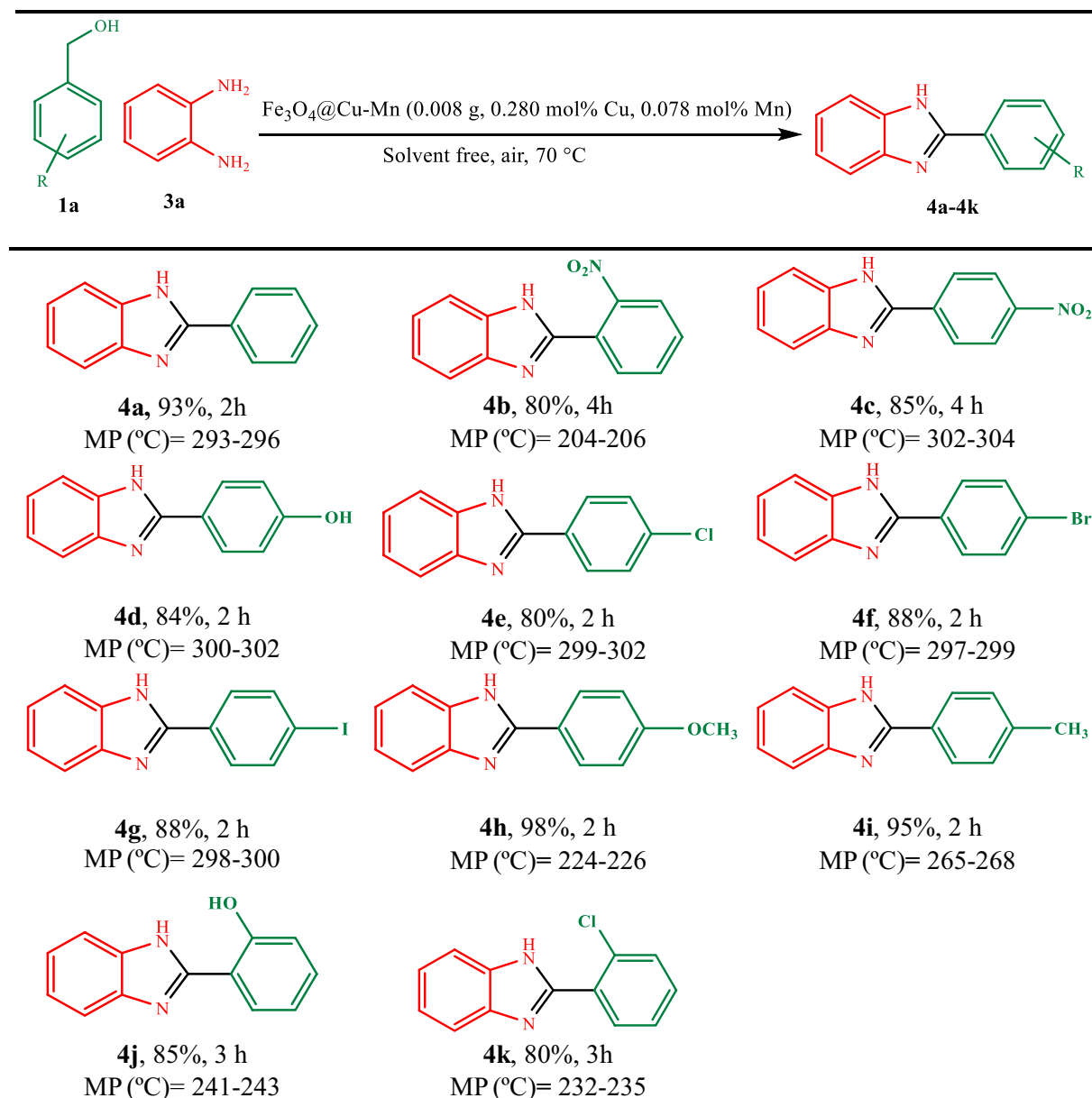


Table 4 Benzimidazole one-pot reaction of on benzyl alcohols with ortho phenylenediamine catalyzed by Fe₃O₄@Cu-Mn. Reaction conditions: Benzyl alcohol (1.2 mmol) and ortho phenylenediamine (1

mmol), Cat. (0.008 g, 0.280 mol% Cu, 0.078 mol% Mn), solvent free, 70 °C, under aerobic condition



proved the homogeneous and spherical morphology of the nanoparticles as same as the fresh one. More importantly, no significant agglomeration was seen in the images (Fig. 9a, b). In addition, the TGA curve of the recovered catalyst was

quite similar to that of the fresh one (Fig. 9c), indicating that the catalyst retained its structure after repeated recovery and reuse.

Table 5 Biginelli one-pot reaction of on benzyl alcohols with ethyl acetoacetate and urea catalyzed by Fe₃O₄@Cu-Mn. Reaction conditions: Benzyl alcohol (1.2 mmol), ethyl acetoacetate (1.2 mmol), and

urea (1 mmol), Cat. (0.008 g, 0.280 mol% Cu, 0.078 mol% Mn), solvent free, 70 °C, under aerobic condition

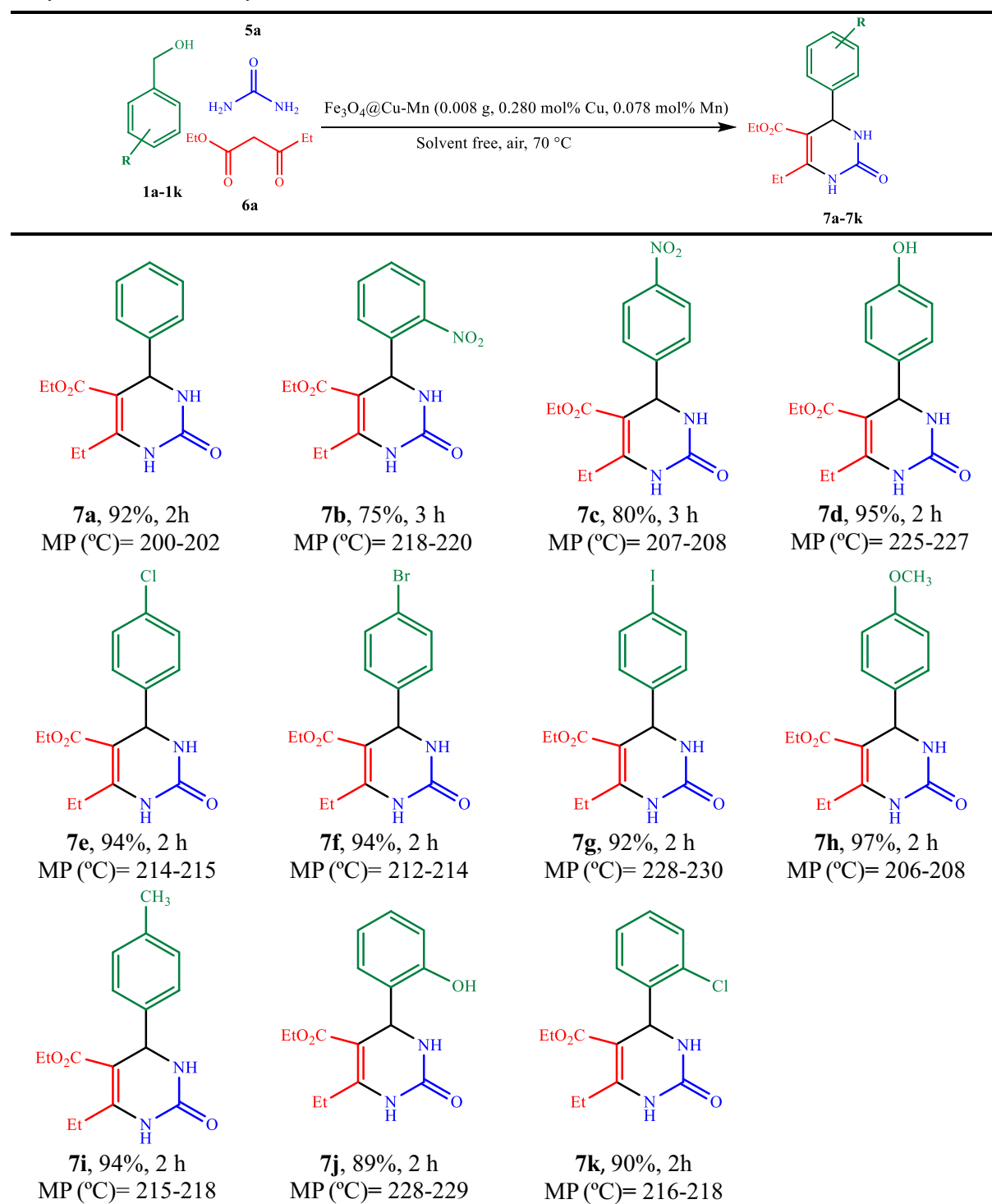


Table 6 Designed control experiments for the oxidation of alcohol, and the one-pot preparation of benzimidazole, and Biginelli reactions

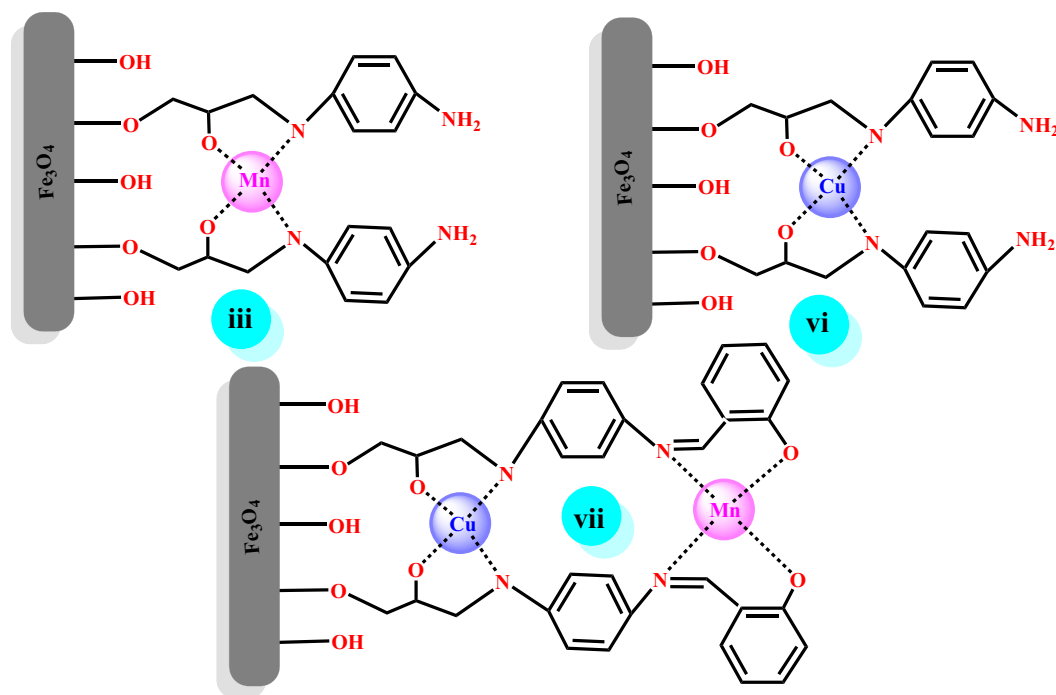
Entry	Catalyst	Oxidation		Biginelli Yield(%)	Benzimidazole Yield (%)
		Yield (%)	Selectivity (%)		
1	Cu(OAc) ₂ ·H ₂ O	15	55	Trace	Trace
2	Mn(OAc) ₂ ·4H ₂ O	25	45	Trace	Trace
3	Fe ₃ O ₄ NPs	–	–	–	–
4	Compound (iii)	55	80	30	30
5	Compound (vi)	35	75	40	35
6	Compound (vii)	80	97	80	85
7	Compound (v)	95	99	93	92
8	Compound (v) ^a	20	99	10	10

^aBenzimidazole model reaction under N₂ atmosphere

4 Conclusion

In summary, a Cu-Mn bimetallic complex decorated on magnetite Fe₃O₄ NPs was prepared and used as an environmentally and economically catalyst for the one-pot oxidative

preparation of benzimidazole and Biginelli derivatives from alcohols as a green protocol under aerobic and mild conditions. The catalyst plays the role of alcohol oxidation as well as condensation/ multicomponent reactions at the same time as a domino-*type* reaction. A wide variety of

**Scheme 3** Structure of **iii**, **vi**, and **vii** compounds as three homologue of the main catalyst (**v**)

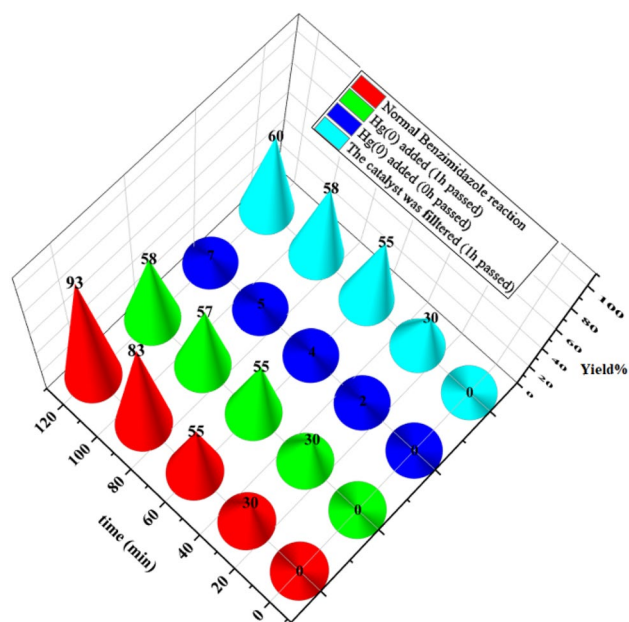


Fig. 7 The results of Hg poisoning and hot filtration tests in the one-pot benzimidazole reaction of benzyl alcohol with *ortho* phenylenediamine

dihydropyrimidinones and benzimidazoles derivatives have been synthesized under optimum conditions with good to high yields. $\text{Fe}_3\text{O}_4@\text{Cu-Mn}$ catalyst was characterized using different techniques such as FT-IR, XRD, TEM, FE-SEM, VSM, EDX, and ICP, analyses. All mentioned analyses emphasized the proposed structure, spherical morphology, being nanoscale, magnetic nature, expected elements, and metal loading respectively. Moreover, data of poisoning and hot filtration experiments demonstrated the heterogeneity nature of the bimetallic catalyst. The control experiments proved that the catalytic activity of the catalyst is unique for the oxidation of domino one-pot preparation of benzimidazole derivatives as well as Biginelli reaction. More importantly, the bimetallic system controls the selectivity of the oxidation and subsequently promotes the following reactions. In this regard, a synergistic effect and cooperative function could be considered for this system. Recycling and recovering studies revealed that the catalyst could be recycled for at least five consecutive runs with reservation of its stability, structure, morphology, and size distribution, that was manifested by TGA, FT-IR, TEM, and FE-SEM analyses over the recovered catalyst.

Scheme 4 The plausible reaction mechanism for the Biginelli and benzimidazole reactions catalyzed by $\text{Fe}_3\text{O}_4@\text{Cu-Mn}$ catalyst

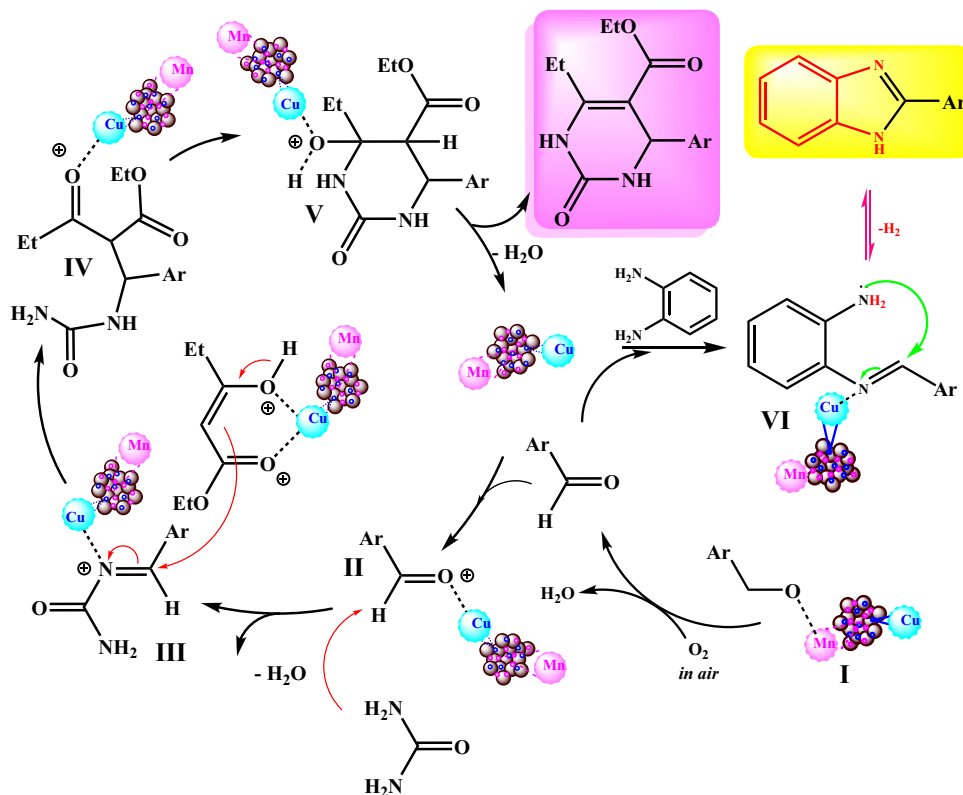
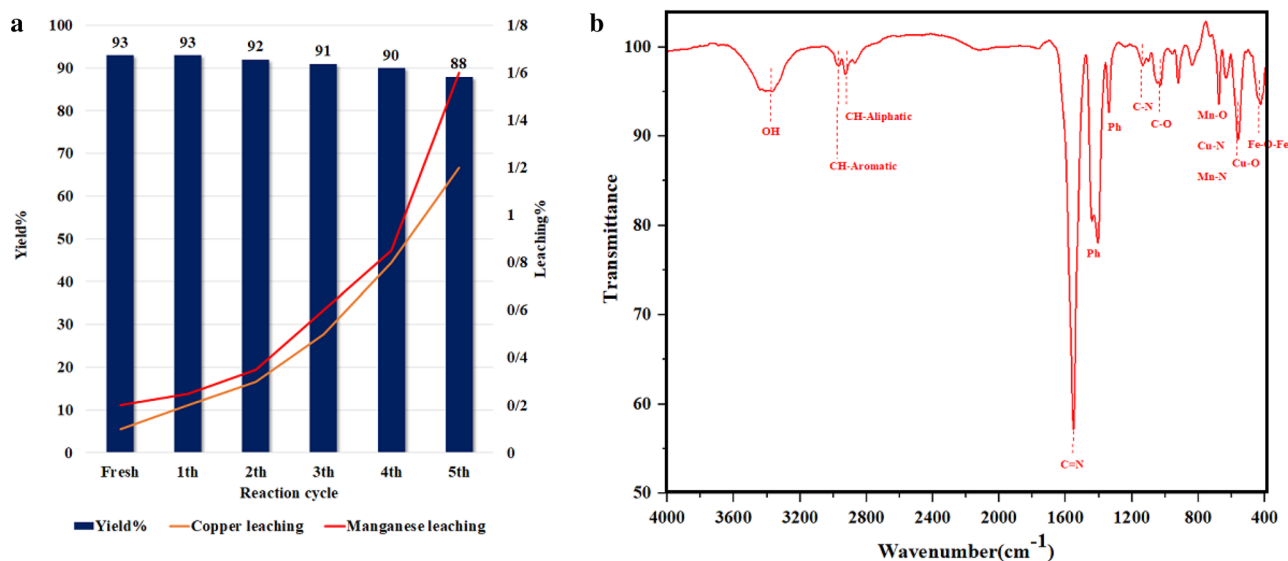


Table 7 Comparison of the Fe_3O_4 @Cu-Mn catalyst activity in the Biginelli and benzimidazole reactions with other one-pot synthesis methods

Entry	Reaction	Catalyst ^{ref}	Solvent	T (°C)	Time (h)	Yield (%)	Ref
1	Benzimidazole ^a	Fe_3O_4 @Cu-Mn	Solvent free	70	2–4	90–98	This work
2 ^b		Ru(II)-PNS(O) pincer	H_2O	165	12	64–85	[69]
3		Cu-Pd/ γ - Al_2O_3	H_2O	180	12	13.9–100	[39]
4 ^c		Ru(II)-NNN pincer	H_2O	165	12	60–97	[70]
5 ^d		Co complex	Toluene	150	24	28–99	[71]
5	Biginelli ^e	Fe_3O_4 @Cu-Mn	Solvent free	70	2–3	75–97	This work
6 ^f		[Hmim]HSO ₄ -NaNO ₃	Solvent free	80	2–6	50–97	[25]
7 ^g		Oxone-KBr-TEMPO	Solvent free	r.t	3.5–4	78–95	[72]

^aBenzimidazole reaction of benzyl alcohol and *ortho* phenylenediamine^bAdditive: NaBPh₄ and Cs₂CO₃^cAdditive: NaBPh₄ and 1,2-bis(diphenyl-phosphanyl)ethane^dAdditive: NaBEt₃H^eBiginelli reaction of benzyl alcohol, ethyl acetoacetate, and urea^f[Hmim]HSO₄: 1-methylimidazolium hydrogen sulphate^gMechanochemical (ball milling) condition**Fig. 8** **a** The recyclability studies of the catalyst for the model benzimidazole reaction (*one-pot method from alcohol*) under optimized conditions. **b** FT-IR analysis of the recovered catalyst after 5th run

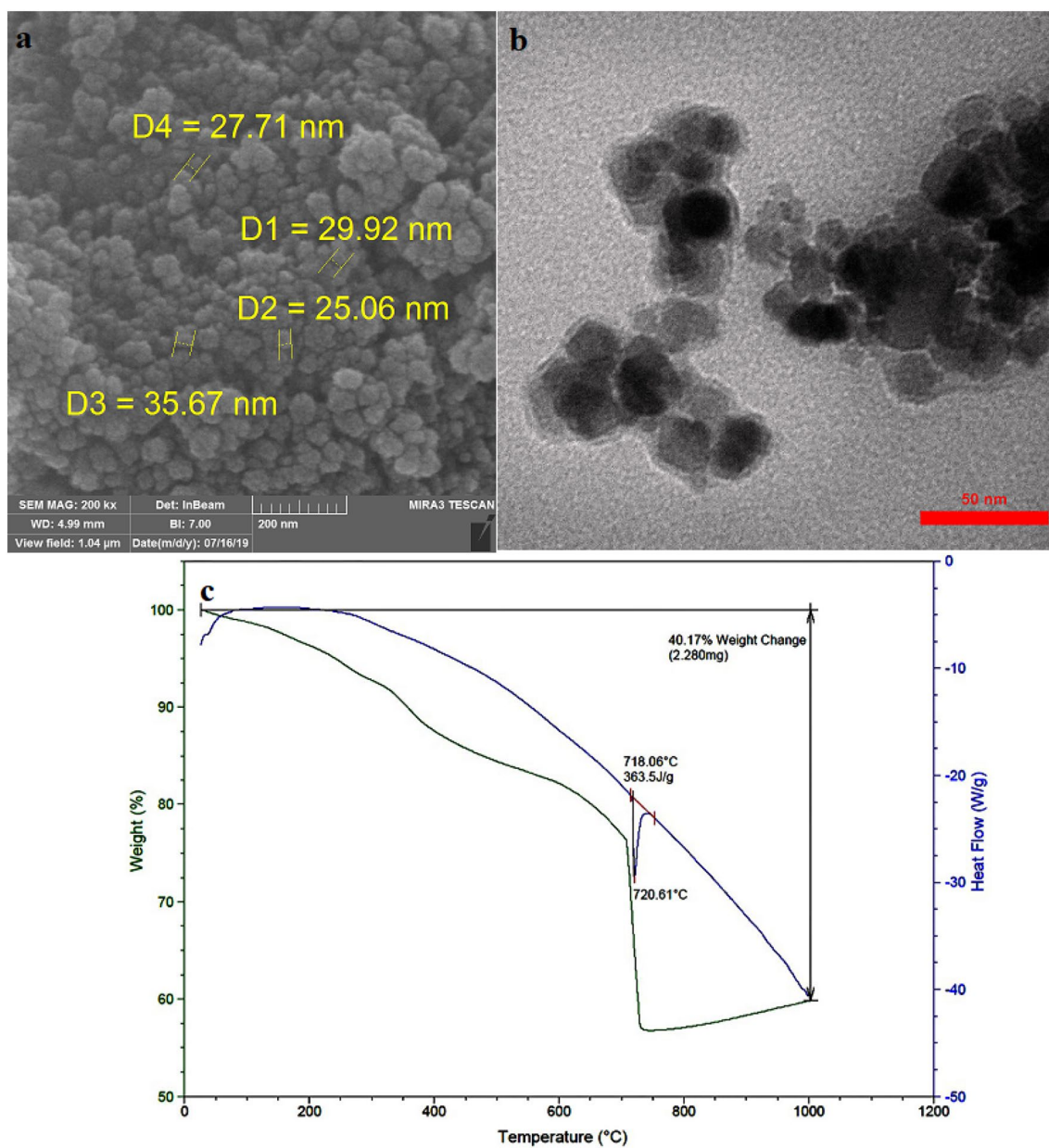


Fig. 9 **a** FE-SEM, **b** TEM, and **(c)** TGA analyses of the recovered catalyst after 5th run for the model benzimidazole reaction (*one-pot method from alcohol*) under optimized conditions

Acknowledgements The authors are grateful to the University of Birjand for financial support.

References

- Alvim HGO, Da Silva Júnior EN, Neto BAD (2014) *RSC Adv* 4:54282–54299
- Slobbe P, Ruijter E, Orru RVA (2012) *Medchemcomm* 3:1189–1218
- Patil RV, Chavan JU, Dalal DS, Shinde VS, Beldar AG, Comb ACS (2019) *Sci* 21:105–148
- Chen XH, Xu XY, Liu H, Cun LF, Gong LZ (2006) *J Am Chem Soc* 128:14802–14803
- Sheykhan M, Yahyazadeh A, Ramezani L (2017) *Mol Catal* 435:166–173
- Ma Y, Qian C, Wang L, Yang M (2000) *J Org Chem* 65:3864–3868
- Bin Bai Y, Zhang AL, Tang JJ, Gao JM (2013) *J Agric Food Chem* 61:2789–2795
- Singh I, Luxami V, Paul K (2019) *Eur J Med Chem* 180:546–561
- Huang ST, Hsei IJ, Chen C (2006) *Bioorganic. Med Chem* 14:6106–6119
- Tong Y, Bouska JJ, Ellis PA, Johnson EF, Leveson J, Liu X, Marcotte PA, Olson AM, Osterling DJ, Przytulinska M, Rodriguez LE, Shi Y, Soni N, Stavropoulos J, Thomas S, Donawho CK, Frost DJ, Luo Y, Giranda VL, Penning TD (2009) *J Med Chem* 52:6803–6813
- Srestha N, Banerjee J, Srivastava S (2014) *IOSR J Pharm* 04:28–41
- Kanwal A, Saddique FA, Aslam S, Ahmad M, Zahoor AF, Mohsin NUA (2018) *Pharm Chem J* 51:1068–1077
- Guan Q, Sun Q, Wen L, Zha Z, Yang Y, Wang Z (2018) *Org Biomol Chem* 16:2088–2096
- Arnold EP, Mondal PK, Schmitt DC, Comb ACS (2020) *Sci* 22:1–5
- Maiti B, Chanda K (2016) *RSC Adv* 6:50384–50413
- Singla P, Luxami V, Paul K (2014) *RSC Adv* 4:12422–12440
- Sharma AS, Kaur H, Shah D (2016) *RSC Adv* 6:28688–28727
- Guo Z, Liu B, Zhang Q, Deng W, Wang Y, Yang Y (2014) *Chem Soc Rev* 43:3480–3524
- Mobley JK, Crocker M (2015) *RSC Adv* 5:65780–65797
- Katsina T, Clavier L, Giffard J-F, da Silva NMP, Fournier J, Tamion R, Copin C, Arseniyadis S, Jean A (2020) *Org Process Res Dev*
- Brioche J, Masson G, Zhu J (2010) *Org Lett* 12:1432–1435
- Miao Z, Luan Y, Qi C, Ramella D (2016) *Dalt Trans* 45:13917–13924
- Bala M, Verma PK, Sharma U, Kumar N, Singh B (2013) *Green Chem* 15:1687–1693
- Hille T, Irrgang T, Kempe R (2014) *Chem—A Eur J* 20:5569–5572
- Garima P, Srivastava VP, Yadav LDS (2010) *Tetrahedron Lett* 51:6436–6438
- Mei Q, Liu H, Yang Y, Liu H, Li S, Zhang P, Han B, Sustain ACS (2018) *Chem Eng* 6:2362–2369
- Rajabimoghadam K, Darwish Y, Bashir U, Pitman D, Eichelberger S, Siegler MA, Swart M, Garcia-Bosch I (2018) *J Am Chem Soc* 140:16625–16634
- Dhakshinamoorthy A, Alvaro M, Garcia H (2011) *ACS Catal* 1:48–53
- Zhao X, Zhou Y, Huang K, Li C, Tao DJ, Sustain ACS (2019) *Chem Eng* 7:1901–1908
- Parmeggiani C, Cardona F (2012) *Green Chem* 14:547–564
- Parmeggiani C, Matassini C, Cardona F (2017) *Green Chem* 19:2030–2050
- Sankar M, Dimitratos N, Miedziak PJ, Wells PP, Kiely CJ, Hutchings GJ (2012) *Chem Soc Rev* 41:8099–8139
- De S, Zhang J, Luque R, Yan N (2016) *Energy Environ Sci* 9:3314–3347
- Lorion MM, Mairand K, Kapdi AR, Ackermann L (2017) *Chem Soc Rev* 46:7399–7420
- Nemygina NA, Nikoshvili LZ, Tiamina IY, Bykov AV, Smirnov IS, LaGrange T, Kaszkur Z, Matveeva VG, Sulman EM, Kiwi-Minsker L (2018) *Org Process Res Dev* 22:1606–1613
- Chen YZ, Zhou YX, Wang H, Lu J, Uchida T, Xu Q, Yu SH, Jiang HL (2015) *ACS Catal* 5:2062–2069
- Katkar SV, Jayaram RV (2014) *RSC Adv* 4:47958–47964
- Hou YL, Sun RWY, Zhou XP, Wang JH, Li D (2014) *Chem Commun* 50:2295–2297
- Feng F, Ye J, Cheng Z, Xu X, Zhang Q, Ma L, Lu C, Li X (2016) *RSC Adv* 6:72750–72755
- Wang Y, Zeng Y, Wu X, Mu M, Chen L (2018) *Mater Lett* 220:321–324
- Pasupathi M, Santhi N, Pachamuthu MP, Alamelu Mangai G, Ragupathi C (2018) *J Mol Struct* 1160:161–166
- Kamijo S, Jin T, Huo Z, Yamamoto Y (2003) *J Am Chem Soc* 125:7786–7787
- Kang YS, Risbud S, Rabolt JF, Stroeve P (1996) *Chem Mater* 8:2209–2211
- Jin FL, Yop Rhee K, Park SJ (2011) *J Solid State Chem* 184:3253–3256
- Saremi SG, Keypour H, Noroozi M, Veisi H (2018) *RSC Adv* 8:3889–3898
- Reddy AS, Mao J, Krishna LS, Badavath VN, Maji S (2019) *J Mol Struct* 1196:338–347
- Kazemnejadi M, Alavi SA, Rezazadeh Z, Nasser MA, Allahresani A, Esmaeilpour M (2019) *J Mol Struct* 1186:230–249
- Vieira AP, Wegermann CA, Da Costa Ferreira AM (2018) *New J Chem* 42:13169–13179
- Rajput S, Pittman CU, Mohan D (2016) *J Colloid Interface Sci* 468:334–346
- Mungse HP, Verma S, Kumar N, Sain B, Khatri OP (2012) *J Mater Chem* 22:5427–5433
- Kazemnejadi M, Alavi SAG, Rezazadeh Z, Nasser MA, Allahresani A, Esmaeilpour M (2019) *Green Chem* 21:1718–1734
- Xuan S, Wang YXJ, Yu JC, Leung KCF (1843) *Langmuir* 25(2009):11835–11841
- Feizpour F, Jafarpour M, Rezaeifard A (2018) *Catal Letters* 148:30–40
- Erasmus E, Niemantsverdriet JW, Swarts JC (2012) *Langmuir* 28:16477–16484
- Nasrollahzadeh M, Nezafat Z, Bidgoli NSS, Shafiei N (2020) *Mol Catal* 484:110775
- Ghafuri H, Joorabchi N, Emami A, Esmaili Zand HR (2017) *Ind Eng Chem Res* 56:6462–6467
- Elhamifar D, Mofatehnia P, Faal M (2017) *J Colloid Interface Sci* 504:268–275
- Kappe CO (2000) *Acc Chem Res* 33:879–888
- Forzatti P, Lietti L (1999) *Catal Today* 52:165–181
- Saha S, Abd Hamid SB (2016) *RSC Adv* 6:96314–96326
- Jeena V, Robinson RS (2015) *Org Biomol Chem* 13:8958–8977
- Li G, Wang J, Yuan B, Zhang D, Lin Z, Li P, Huang H (2013) *Tetrahedron Lett* 54:6934–6936
- Diarjani ES, Rajabi F, Yahyazadeh A, Puente-Santiago AR, Luque R (2018) *Materials (Basel)* 11
- Rezaei N, Ranjbar PR (2018) *Tetrahedron Lett* 59:4102–4106
- Zeynizadeh B, Rahmani S, Eghbali E (2019) *Polyhedron* 168:57–66
- Alshammari A, Kalevaru VN, Martin A (2016) *Catalysts* 6
- Hamid S, Kumar MA, Lee W (2016) *Appl Catal B Environ* 187:37–46

68. Besenbacher F, Chorkendorff I, Clausen BS, Hammer B, Molenbroek AM, Nørskov JK, Stensgaard I (1998) *Science* 279:1913–1915
69. Luo Q, Dai Z, Cong H, Li R, Peng T, Zhang J (2017) *Dalt Trans* 46:15012–15022
70. Li L, Luo Q, Cui H, Li R, Zhang J, Peng T (2018) *ChemCatChem* 10:1607–1613
71. Daw P, Ben-David Y, Milstein D (2017) *ACS Catal* 7:7456–7460
72. Sahoo PK, Bose A, Mal P (2015) *Eur J Org Chem* 2015:6994–6998
73. Sobhani S, Hosseini Moghadam H, Skibsted J, Sansano JM (2020) *Green Chem* 22:1353–1365

Publisher's Note Springer Nature remains neutral with regard to jurisdictional claims in published maps and institutional affiliations.

Affiliations

Mohammad Ali Nasseri¹ · Zinat Rezazadeh¹ · Milad Kazemnejadi¹ · Ali Allahresani¹

¹ Department of Chemistry, Faculty of Sciences, University of Birjand, Birjand 97175-615, Iran